BUTTERWORTH HEINEMANN

Polymer Vol. 36 No. 19, pp. 3745–3752, 1995

0032-3861/95/$10.00 + 0.00

Amphiphilic heteroarm star copolymers of polystyrene and poly(ethylene oxide)*

C. Tsitsilianis† and D. Papanagopoulos
Department of Chemical Engineering, University of Patras, 26500 Patras, Greece

and P. Lutz
Institute Charles Sadron (CRM-EAHP)(CNRS-ULP), 6 rue Boussingault, 67083 Strasbourg cedex, France
(Received 21 March 1994; revised 3 January 1995)

Amphiphilic heteroarm star copolymers bearing polystyrene (PS) and poly(ethylene oxide) (PEO) branches have been synthesized by sequential anionic 'living' copolymerization. These samples have been characterized adequately and shown to exhibit rather well-defined structures. The functionality of the stars is influenced mainly by the molar ratio of divinylbenzene per living ends and the molecular weight of the linear PS precursor. These star copolymers exhibit association phenomena not only in water but also in tetrahydrofuran, which is not a selective solvent for the different arms. Finally, it has been shown that the PEO arms can be crystallized, forming well-defined spherulites. This ability is strongly affected by the PEO content and the thermal history of the samples.

(Keywords: amphiphilic heteroarm star copolymers; polystyrene–poly(ethylene oxide); anionic polymerization; micelles; crystallinity

INTRODUCTION

Model macromolecules exhibiting complex architecture have combined properties, and therefore may be useful in specific applications. New model polymers, named heteroarm star copolymers, of the type A_nB_n (with n up to 17) have recently been synthesized by sequential anionic 'living' copolymerization[1,2]. These polymeric species comprise a central core carrying equal numbers of two different kinds of branches.

Their synthesis involves three steps. In the first step a living polymer precursor is formed, which is subsequently used to initiate the polymerization of a small amount of a suitable bis-unsaturated monomer (i.e. divinylbenzene). A living, star-shaped polymer is formed, bearing within its core a number of active sites that is equal to the number of its branches. In the third step, these active sites are used to initiate the polymerization of another monomer of suitable electroaffinity. New branches (of a different kind) then grow from the core, yielding the heteroarm star copolymer (*Scheme 1*).

The same kind of model macromolecules but with limited functionality have been prepared by a similar method. Polystyrene and polybutadiene star polymers of the type A_2B_2 were synthesized using 1,3-bis(1-phenylvinyl)benzene[3] as the linking agent. In another attempt, diblock macromonomers with a central unsaturation were used for the synthesis of A_nB_n type block copolymers. The method used for the polymerization of these macromonomers was either free-radical homopolymerization[4] or addition-condensation of diblock copolymer films with sulfur monochloride[5]. The chlorosilane approach[6] has also been used for the synthesis of A_2B_2, ABC and ABCD type star-shaped block copolymers[7,8].

Kanaoka *et al.*[9] extended the three-step procedure described previously and synthesized A_nB_n type star copolymers by using living cationic copolymerization. By end-capping of the second-generation arms and using n.m.r. analysis, they showed that the initiation of the second monomer from the living sites located in the core is quantitative. Furthermore, upon hydrolysis of the ester functions of the second generation of arms, amphiphilic star copolymer can be obtained.

Our efforts to synthesize amphiphilic heteroarm star copolymers by anionic polymerization began with the preparation of polystyrene–poly(t-butyl acrylate) samples (PS_nPtBA_n)[2,10]. As is known, the PtBA branches can be easily hydrolysed to yield the corresponding poly(acrylic acid) branches. The present work is devoted to the synthesis and characterization of amphiphilic heteroarm star copolymers with hydrophobic branches of polystyrene and hydrophilic branches of poly(ethylene oxide) (PEO), the latter being a non-ionic, water soluble polymer. Preliminary results have already been reported[11]. It should be mentioned that similar polymeric species have been prepared by Berlinova *et al.*, but with very low functionality[4].

An interesting feature of the three-step method is that the second-generation arms growing from the core are

* Part of this work was presented at the 'Polymer Conference', held at Cambridge, UK, in July 1993
† To whom correspondence should be addressed

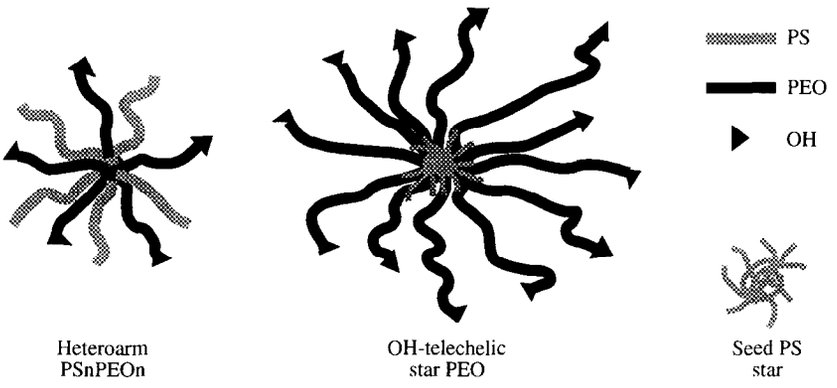

Scheme 1

fitted with anionic sites at their outer ends that can be easily functionalized. Thus, by choosing very short PS branches, this method can be used for the synthesis of telechelic star-shaped polymers[10]. An example of such polymeric species is PEO star polymers bearing terminal OH functions (*Scheme 1*). An alternative method, the so-called 'core-first' method, has been applied for the synthesis of PEO star polymers[12]. These two processes are compared and discussed in a recent article[11].

An additional interest for PS_nPEO_n star molecules arises from the fact that PEO is a crystallizable polymer. In this work, the ability of the PEO branches to crystallize has been investigated by means of differential scanning calorimetry (d.s.c.) and microscopy.

EXPERIMENTAL

Solvents and monomers were purified according to classical procedures. Cumyl potassium was purchased from Orgment as a suspension in heptane. Further treatment was carried out under argon atmosphere to obtain it in tetrahydrofuran (THF) solution. The initiator was titrated by the acetanilide method prior to use.

Synthetic procedure

The synthesis was performed in a gas-tight reactor under a small over-pressure of argon[9]. In the first step, a known amount of cumyl potassium was used to initiate the polymerization of styrene at −40°C in THF, yielding the PS precursor. After consumption of the monomer an aliquot of the reaction medium was sampled out for characterization of the PS branches. In the second step, polystyryl potassium was used to initiate the polymerization of a known amount of divinylbenzene (DVB). The DVB was added to the reaction medium under vigorous stirring at about −40°C, the $[DVB]/[K^+]$ mole ratio ranging from 3 to 10. Once polymerization of the DVB was complete, a small amount of the solution containing the 'seed' PS star molecules was sampled out for the purpose of characterization. Subsequently, in the third step, a chosen amount of oxirane was added to the reaction medium at −30°C under slight vacuum. The temperature was then increased progressively to 30–35°C and was maintained at that level for about 24 h to ensure completion of the oxirane polymerization. The reaction mixture was then deactivated and the heteroarm star polymer was recovered by precipitation in cold ether, or in cold heptane in the case of samples with high PS contents.

Characterization

The weight-average molecular weights M_w were determined by light scattering (LS) in THF using a model SEM RD spectrogoniometer (Sematech, France) equipped with a He–Ne laser (633 nm).

The refractive index increments dn/dc were measured in THF by means of a Chromatic KMX-16 differential refractometer operating at 633 nm.

Gel permeation chromatography (g.p.c.) was performed using a model 201 apparatus equipped with a model 401 differential refractometer as detector (Waters Associates). Two different series of columns were employed during the experiments, depending upon the nature of the mobile phase. With THF as eluent a set of four μ-Styragel columns (10^3, 10^4, 10^5 and 10^6 Å) was used, while for aqueous g.p.c. two Shodex columns of type OH, pack B-805 and B-804, were employed. In both cases the flow rate was 1 $cm^3\,min^{-1}$.

Differential scanning calorimetry was performed using a Du Pont 910 calorimeter equipped with a 99 thermal analyser. The instrument was calibrated with a sapphire (Al_2O_3) standard. The heating rate was 10°C min^{-1} and the experiments were carried out under a nitrogen atmosphere.

An Olympus BH2 optical microscope, fitted with crossed nicols, was used to visualize the crystallization of the PEO branches.

RESULTS AND DISCUSSION

Each synthesis yielded three kinds of sample: the linear PS precursor (lPS), the 'seed' PS star (sPS) and the heteroarm star copolymer designated as PS_nPEO_nx, where n is the number of arms of either kind and x the weight content of PEO.

Characteristic g.p.c. chromatograms obtained with THF as the eluent and Styragel columns are shown in *Figure 1*. The traces for the star PS show that a small amount of the linear PS precursor remains unattached to the DVB cores. The fact that the position of the peak corresponding to the lPS does not shift to lower retention volumes upon the addition of oxirane (see PS_nPEO_n chromatogram) demonstrates that most of the remaining linear precursor arises from accidental deactivation during the DVB polymerization.

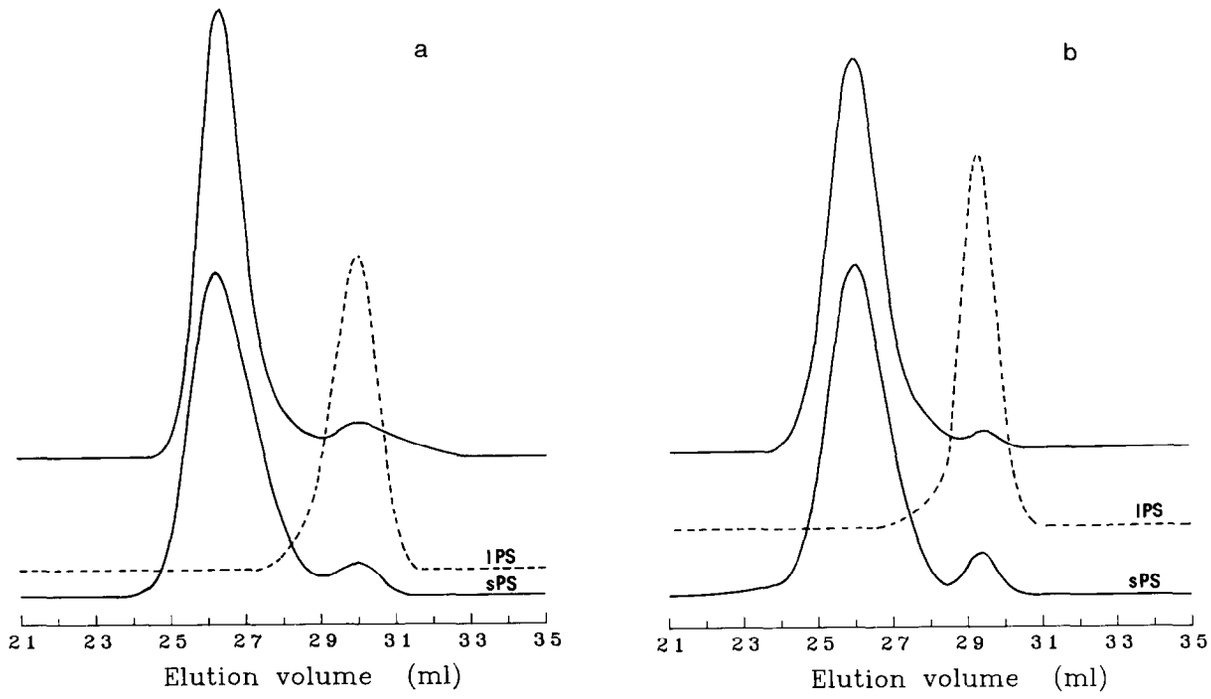

Figure 1 G.p.c. chromatograms of PS_nPEO_n heteroarm star copolymers and their respective precursors: (a) PS_9PEO_923; (b) PS_8PEO_839

Another interesting observation from *Figure 1* is that the retention volumes of the star PS and the heterostar copolymer coincide, confirming that the oxirane polymerization is initiated by the living sites located in the DVB cores of the 'seed' PS star. It is known[13] that the hydrodynamic volume of star-shaped macromolecules is practically independent of the number of arms, beyond a certain value of n. Therefore, if the effective size of the PEO arms is smaller than that of the PS arms, and provided the contribution of interactions between arms of different nature is negligible[2], the hydrodynamic volume of the star molecule will be determined primarily by the size of the PS arm. The effective size of the arms in dilute solution can be expressed[14] by the end-to-end distance $(\overline{r^2})^{1/2}$

$$(\overline{r^2})^{1/2} = \Phi^{-1/3}\{[\eta]M\}^{1/3} \quad (1)$$

where Φ is a universal constant often taken as 2.6×10^{23} cm^3 g^{-1}, $[\eta]$ is the intrinsic viscosity and M the molar mass.

Rearranging $[\eta]$ from the Mark–Houwink–Sakurada (MHS) equation, we obtain

$$(\overline{r^2})^{1/2} = \Phi^{-1/3}[KM^{a+1}]^{1/3} \quad (2)$$

where K and a are the MHS constants. As shown in *Table 1*, in both samples the effective size of the PS arms is greater than that of PEO arms, confirming the above assumptions.

Table 1 End-to-end distance of PS_nPEO_n arms

Sample	Arm	M_{br}[a]	$K \times 10^{2}$[b]	a[b]	$(\overline{r^2})^{1/2}$ (Å)
PS_9PEO_923	PS	22000	1.6[c]	0.706[c]	116.35
	PEO	6500	4.4[d]	0.655[d]	70.19
PS_8PEO_839	PS	15000	1.6	0.706	93.58
	PEO	9100	4.4	0.655	84.51

[a] Values from *Table 2*
[b] MHS constants
[c] From ref. 15
[d] From viscosity measurements of PEO standards in THF at 25°C

It is noted that samples with high PEO contents are strongly retained by the column packing (Styragel), due to absorption effects.

The chromatograms of the 'seed' PS star were analysed by a deconvolution program to determine the amount of linear PS precursor left in the samples[1]. The weight-average molecular weights of the unfractionated sPS samples were obtained by light scattering. Then, the proportion of lPS precursor left in the sample was used to obtain corrected values that could be used to determine the functionality f (number of PS branches) of the sPS molecules. Taking into account the weight of the cores, f can be calculated by the formula

$$f = \frac{M_{w,PS^*}}{M_{w,pr} + m_0[DVB]/[LE]} \quad (3)$$

where [DVB]/[LE] is the mole ratio of DVB to living ends, m_0 is the molecular weight of the DVB monomer, and M_{w,PS^*}, $M_{w,pr}$ are the molecular weights of the sPS and lPS, respectively. It should be mentioned here that f is an average value as molecular polydispersity is expected to exist in these samples, arising from fluctuations in the size of the DVB cores.

The characterization data are summarized in *Table 2*. The two main experimental factors that determine f are the [DVB]/[LE] mole ratio and the molecular weight of the precursor, with the former playing the major role. In fact, as shown in *Figure 2a*, keeping all other factors constant, f increases with [DVB]/[LE] ratio. On the other hand, f decreases with the molecular weight of the linear precursor and this phenomenon is more pronounced in the low molecular weight range (*Figure 2b*), as it arises from steric hindrance effects.

The overall molecular weights of the heteroarm star

Table 2 Characterization data on heteroarm star copolymers

Sample	$M_{w,pr} \times 10^{-3}$ (g.p.c.)	[DVB]/[LE]	% IPS left	$M_{w,PS^-} \times 10^3$ (LS)	$M_{w,PS^*} \times 10^{-3}$ (corrected)	W_{PEO} (%)	$M_{w,PS_nPEO_n} \times 10^{-3}$ (calc.)[a]	$M_{br,PEO} \times 10^{-3}$ (calc.)[b]	$M_{w,PS_nPEO_n} \times 10^{-3}$ (LS)	f[c]
PS_9PEO_923	22	10	8	189	203.5	23	245.5	6.5	280	8.7
PS_8PEO_819	27	5	16	195	227	19	241	5.6	252	8.2
PS_8PEO_839	15	5	8.5	114	123.2	38.5	185.5	9.1	182.5	7.9
$PS_{15}PEO_{15}86$	3	5	2	55	56	86	393	22.5	339	15.3
$PS_{19}PEO_{19}78$	3	7.6	3	74.7	76.9	78	339.6	14.2	182	19.3
$PS_{11}PEO_{11}86$	3	3	4	37	38.4	86	264	21.2	190	11.3

[a] Calculated values using equation (4)
[b] Calculated values using equation (6)
[c] f is the average number of each kind of arm

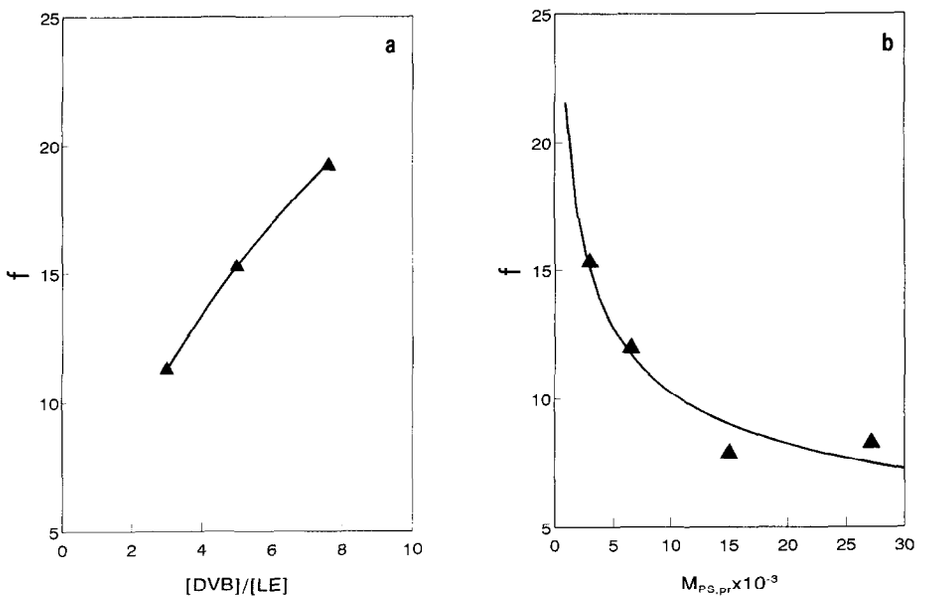

Figure 2 Functionality f of 'seed' PS stars as a function of (a) ratio [DVB]/[LE] and (b) molecular weight of PS precursor

copolymers were measured by light scattering in THF. For samples with low PEO content (<40%), the experimental values are very close to those calculated from the corresponding M_{w,PS^*} values and the weight content of PEO in the heteroarm star copolymers, W_{PEO}, according to

$$M_{w,PS_nPEO_n} = \frac{M_{w,PS^*}}{1 - W_{PEO}} \quad (4)$$

On the contrary, there is no agreement in the case of samples with high PEO content, probably because of the association phenomena discussed below.

The three-step procedure described herein allows estimation of the molecular weight of the second-generation arms, which cannot be measured directly. The average molecular weight of the individual PEO arms can be calculated according to the formula

$$M_{br,PEO} = \frac{M_{w,PS_nPEO_n} - M_{w,PS^*}}{f} \quad (5)$$

provided no accidental deactivation of the active sites within the cores of the seed PS stars has taken place. Furthermore, access of the second monomer to the active sites must not be prohibited or impeded by the steric hindrance arising from the PS arms. The fact that rapid decoloration of the reaction medium takes place upon the addition of oxirane shows that access to the sites is provided.

Substituting for M_{w,PS_nPEO_n} from equation (4) we can write

$$M_{br,PEO} = \frac{M_{w,PS^*} W_{PEO}}{f(1 - W_{PEO})} \quad (6)$$

Values of $M_{br,PEO}$ have been calculated from equation (6) to avoid problems (association effects) arising from the direct determination of M_{w,PS_nPEO_n} and are collected in *Table 2*. Let us comment on the case of sample PS_8PEO_839. The effective size of the PEO arms is approximately equal to that of the PS arms. If the number of PEO arms were lower, owing to the reasons mentioned above, the molecular weight of the PEO arms and therefore their effective size in the solution should be higher. This should provoke a shift in the elution volume of the heteroarm star, with respect to that of the seed PS star, towards lower values. Since this is not the case (*Figure 1*), the assumption used for the derivation of equation (6) can be considered valid.

Association effects

Surprisingly, in these samples, strong association

phenomena are observed by light scattering in THF, even though this solvent is not very selective for the constituents of the copolymer.

Consider the light scattering data from dilute solutions of $PS_{15}PEO_{15}86$ in THF at 30°C. The angular

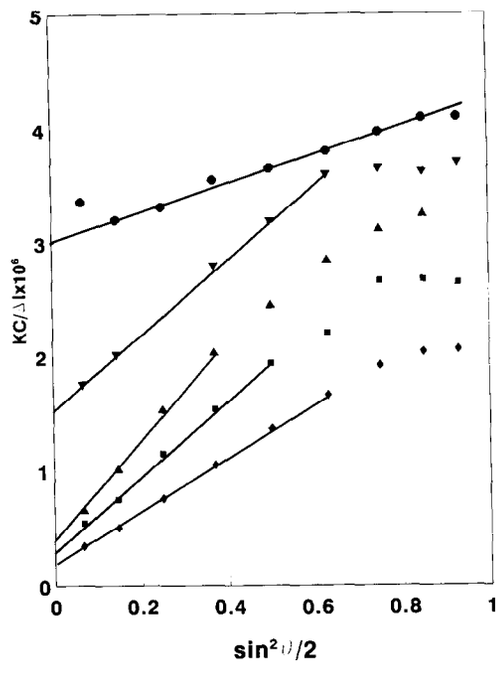

Figure 3 Dependence of $KC/\Delta I$ (mol g^{-1}) on $\sin^2\Theta/2$ for $PS_{15}PEO_{15}86$ in THF at 30°C at different concentrations, c (g cm^{-3}): ●, 0.1364×10^{-3}; ▼, 0.2182×10^{-3}; ▲, 0.2182×10^{-2}; ■, 0.3636×10^{-3}; ◆, 0.7273×10^{-3}

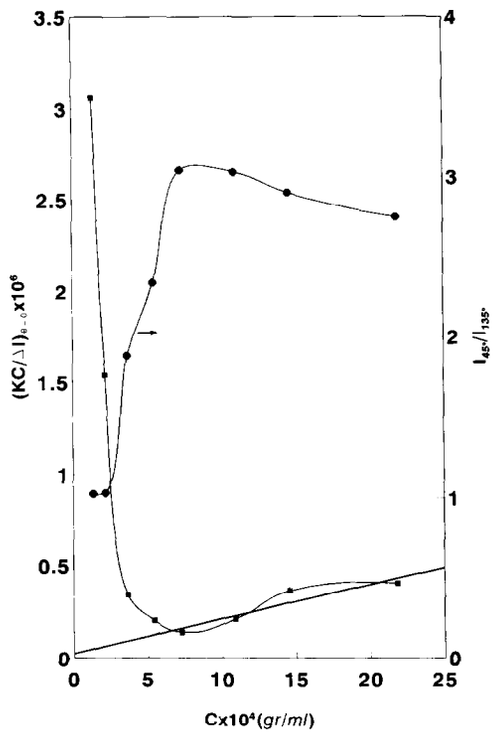

Figure 4 Concentration dependences of $(KC/\Delta I)_{\theta=0}$ (mol g^{-1}) and disymmetry factor z for $PS_{15}PEO_{15}86$ in THF at 30°C

dependence of the inverse scattering intensity $KC/\Delta I$ is plotted for various concentrations C in *Figure 3*. These scattering envelopes reveal association phenomena, as the non-linear curves observed can be attributed to the existence of an equilibrium between micelles and unimers. At low angles it is possible to get linear extrapolations and values of $(KC/\Delta I)_{\theta=0}$ are plotted against concentration in *Figure 4*. The shape of this curve suggests that the system exhibits behaviour similar to the associations observed in block copolymers in a selective solvent[16–18]. In fact, as the concentration of the solution increases, an abrupt decrease of $(KC/\Delta I)_{\Theta=0}$ is observed accompanied by an abrupt increase of the disymmetry factor z (ratio of the scattered light intensities at angles of 45 and 135°), indicating the formation of polymolecular aggregates.

At higher concentrations the $(KC/\Delta I)_{\Theta=0}$ *versus* C plot becomes linear with a positive slope. In this range it seems that the equilibrium between micelles and unimers is predominantly in favour of micelles. Assuming that free remaining unimers do not contribute significantly to the scattered intensity, the apparent molecular weight of the micelle can be estimated from the intercept

$$(KC/\Delta I)_{\Theta=0,\,C=0} = 1/M_w^{app} \qquad (7)$$

The obtained value of M_w^{app} for the micelles is 4.66×10^7 (g mol^{-1}), two orders of magnitude higher than the molecular weight of the unimer, indicating high association number N. However, N cannot be determined accurately owing to experimental uncertainty.

Strong micellization phenomena are also observed in aqueous solutions. The $PS_{15}PEO_{15}86$ is soluble in water with the aid of a small amount of THF. When the THF is removed from the solution by evaporation, the star copolymers remain soluble. G.p.c. with two Shodex columns showed one single peak of low polydispersity in the high molecular weight exclusion limit ($> 10^6$ g mol^{-1}). This observation suggests that polymolecular aggregates are formed, as expected, owing to the amphiphilic character of these heteroarm star-shaped macromolecules. All these association phenomena are being studied in detail and will be reported in a forthcoming paper.

Crystallinity behaviour

Heteroarm star copolymers are a type of block copolymer and, if the thermodynamic (polymer–polymer interaction parameter) and structural (M_w of the different arms) conditions are favourable, they exhibit microphase separation in the bulk as has been shown theoretically[19] and experimentally[20]. It is well known that PS and PEO are incompatible and their block copolymers form crystallizable PEO-rich domains and amorphous PS-rich domains. In the following paragraphs, we deliver some preliminary results concerning the crystallinity behaviour of PS_nPEO_n star copolymers.

D.s.c. experiments were performed on all samples several times, under different thermal histories. The first run was carried out on samples as received, after prolonged drying, in the range from 0 to 130°C with a heating rate of 10°C min^{-1}. All the samples exhibited melting endotherms in the vicinity of 60°C. It is noted that samples with low PEO content (PS_9PEO_923 and PS_8PEO_819) exhibited two melting endotherms, one near 60°C and another about 15°C lower.

Table 3 Melting behaviour of PS_nPEO_n star copolymers

	Thermal history[a]								
	[A]		[B]		[C]		[D]		
Sample	T_m (°C)	ΔH_f (J g^{-1})	T_m (°C)	ΔH_f (J g^{-1})	T_m (°C)	ΔH_f (J g^{-1})	T_m (°C)	ΔH_f (J g^{-1})	X_c (%)
PS_9PEO_923	44, 58	49.9	–	–	52, 59	85.7	38, 52	100.5	49
PS_8PEO_819	41, 57	131.6	–	–	58	139.3	51	82.0	40
PS_8PEO_839	59	74.85	59	58.7	57	57.3			
$PS_{15}PEO_{15}86$	60	117.27	59	105.85	62	113.5	61.5	126.3	61.6
$PS_{19}PEO_{13}78$	61	116.42	60	100.1	61	107.5	61	139.4	68
$PS_{11}PEO_{11}86$	59	112.22	57	90.12	58	88.7	59.5	133.1	65

[a] Thermal histories as follows: A – as received, quenched to 0°C, run 10°C min^{-1}; B – 130°C (10 min), quenched to 0°C (10 min), run 10°C min^{-1}; C – 130°C (10 min), quenched to −80°C, run 10°C min^{-1}; D – 80°C (10 min), quenched to 25°C (24 h), run 10°C min^{-1}

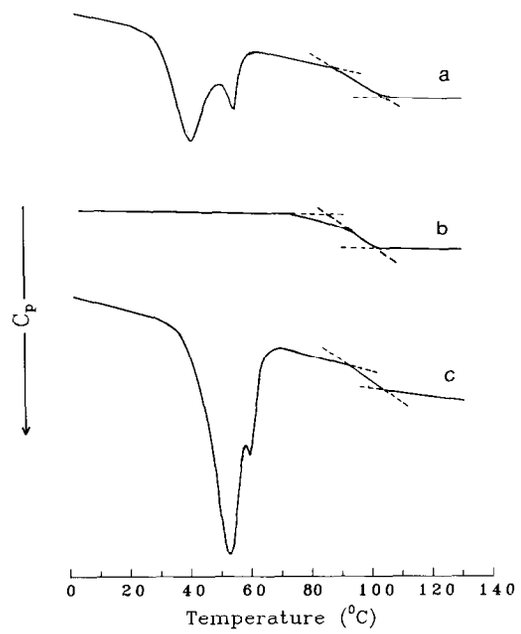

Figure 5 DSC thermograms for PS_9PEO_923 with different thermal histories: (a) 80°C (10 min), quenched to 0°C (10 min); (b) 130°C (10 min), quenched to 0°C (10 min); (c) 130°C quenched to −80°C

The samples were then quenched to 0°C and, after 10 min, a second run was performed. Melting endotherms were again seen at about the same melting temperature (T_m) as before, with the exception of samples PS_8PEO_819 and PS_9PEO_923. In these samples no melting endotherms were observed even after annealing for many hours at any temperature between 0 and 60°C.

Finally, the samples were heated to 130°C for 10 min, then quenched to −80°C and a d.s.c. run was performed. Values of T_m and the enthalpies of fusion per unit mass of PEO in the copolymer (ΔH_f) are gathered in *Table 3* for the samples with the different thermal histories. As can be seen, the PS_8PEO_819 and PS_9PEO_923 samples recover their crystallinity when they are quenched to −80°C. Characteristic thermograms concerning this effect are given in *Figure 5*.

It is very interesting to examine the glass transition behaviour of the glassy PS phase. We have considered three parameters: the onset of the glass transition region, $T_{g,ons}$, defined as the intersection of the extrapolated baseline below the glass transition temperature (T_g) and the line drawn through the inflection step at the heat capacity (C_p) change; T_g itself at half the step change in C_p; and the width of the glass transition region, ΔT_g, which is the temperature difference between the points where the tangent to the inflection intersects the extrapolated baselines above and below T_g. Values of these parameters relating to the thermograms of *Figure 5* are summarized in *Table 4*.

Table 4 Glass transition behaviour of the PS-rich phase of sample PS_9PEO_923

Thermal history	$T_{g,ons}$ (°C)	T_g (°C)	ΔT_g (°C)
80°C (10 min) quenched to 0° (10 min), d.s.c. run	91	99	13
130°C (10 min) quenched to 0° (10 min), d.s.c. run	84	94	18
130°C (10 min) quenched to −80°C, d.s.c. run	91	98	12

In the cases of samples that lose their crystallinity, $T_{g,ons}$ and T_g of the PS phase are shifted towards lower temperatures while the width of the T_g region becomes broader as ΔT_g increases. Similar phase interactions have been observed in PEO–PS–PEO triblock copolymer[21], and suggest that partial mixing between the two phases has taken place. When the samples are cooled to −80°C they recover their crystallinity and phase mixing is completely eliminated, as revealed by the fact that the T_g parameters exhibit the values they had at the first thermal history. The above results suggest that samples of low PEO content heated to 130°C cannot be crystallized in the usual temperature range, at low supercoolings. This phenomenon is related to the partial mixing of the two phases revealed by the T_g depression of PS and broadening of the T_g range. This implies that the resulting structure does not favour the heterogeneous nucleation taking place at low supercoolings, that has been reported for diblock PS–PEO copolymers[22]. The samples crystallize at higher supercooling ($T_c - 20$°C) where some kind of homogeneous nucleation can be induced[22,23]. Once the crystallinity of the samples has been recovered the partial phase mixing is eliminated.

The overall crystallinity of all samples has been determined by heating to 80°C, quenching to 25°C and keeping them at that temperature for 24 h. The degree of crystallinity of the PEO phase was calculated by the equation

$$X_c = \Delta H_f / \Delta H_f^0 \quad (8)$$

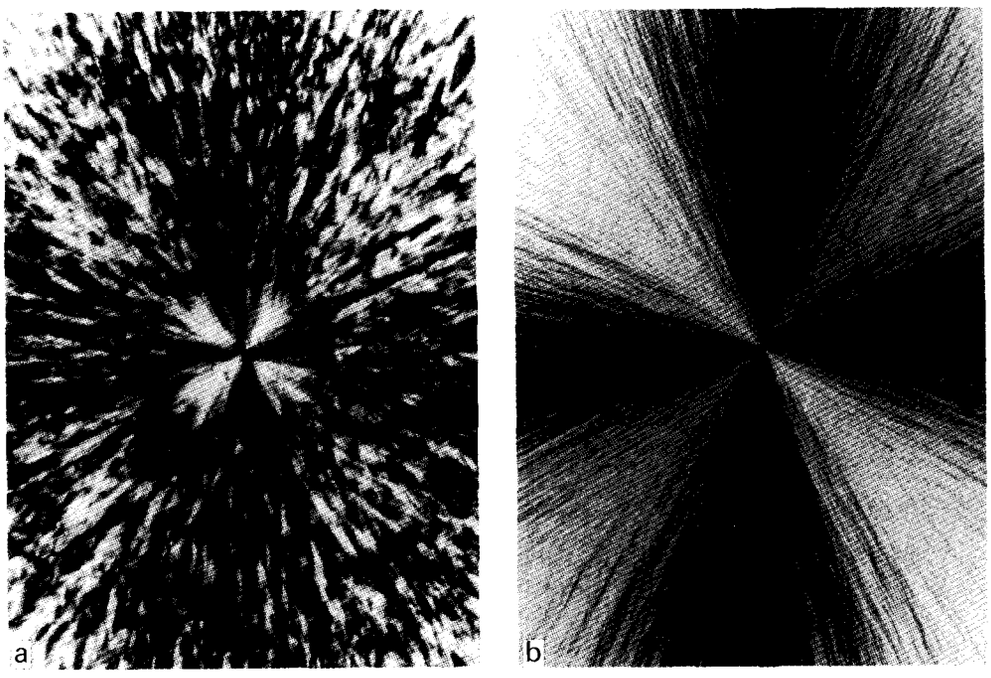

(a) (b)

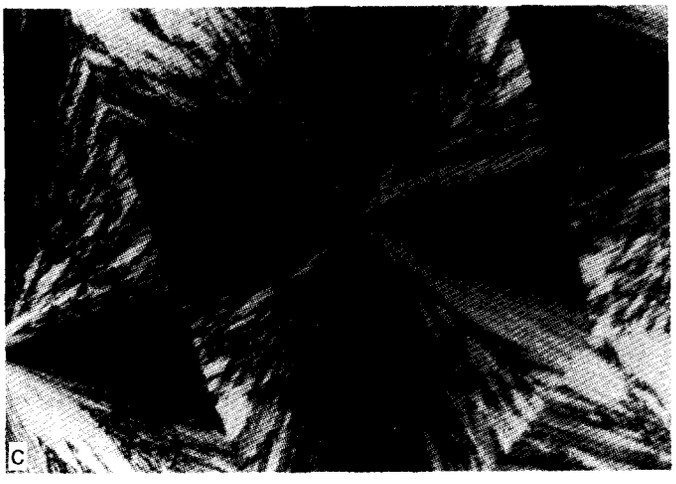

(c)

Figure 6 Optical micrographs of thin films of PS_nPEO_n heteroarm star copolymers cast from nitromethane: (a, b) $PS_{19}PEO_{19}78$; (c) $PS_{15}PEO_{15}86$

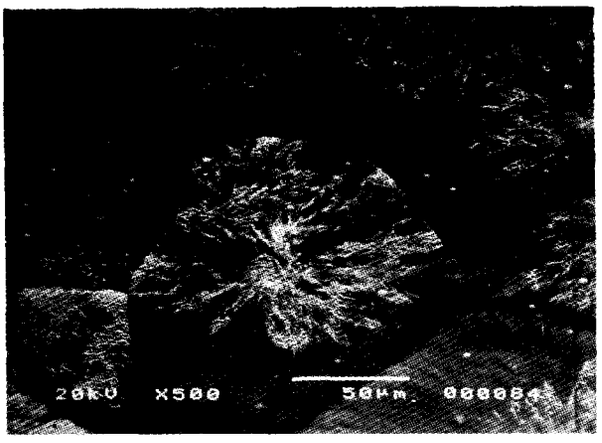

Figure 7 Scanning electron micrograph of $PS_{19}PEO_{19}78$ film cast from nitromethane

where ΔH_f is the enthalpy of fusion per unit mass of the PEO in the copolymer and ΔH_f^0 is the enthalpy of fusion of 100% crystalline PEO ($\Delta H_f^0 = 205\,J\,g^{-1}$)[24]. Values are reported in *Table 3*.

Morphological studies were performed on thin films cast from nitromethane (preferential solvent for PEO) at room temperature, by optical and electron microscopy. *Figure 6* shows some characteristic micrographs of samples with high PEO contents, obtained by polarized light microscopy. Two types of spherulitic texture can be seen, one being more fibrillar. These textures may appear together in the same sample; *Figure 6c* shows that both textures are present in the same spherulite in a sample of $PS_{15}PEO_{15}86$.

Figure 7 is a scanning electron micrograph of $PS_{19}PEO_{19}78$ film cast from nitromethane. It shows clearly a filled space of spherulites, characterized by fibrillar radial growth from a central nucleation source, truncated by impingement.

These preliminary studies demonstrate that the crystalline structure of PS_nPEO_n heteroarm star copolymers resembles, to a first approximation, that appearing in PS–PEO block copolymers[25]. Even though the PEO arms are immobilized at one end, being linked to the core of the star molecule, it seems that they have the ability to be folded and therefore to form the crystalline structures observed previously.

A more detailed analysis is in progress of the crystallinity behaviour of these copolymers with this novel architecture. One of the tasks is to compare their behaviour with that of block copolymers, in an attempt to elucidate possible influences of the macromolecular architecture.

CONCLUDING REMARKS

The three-step living anionic polymerization method developed recently has been applied to the preparation of various amphiphilic polystyrene–poly(ethylene oxide) heteroarm star copolymers. These samples have been characterized adequately and shown to exhibit rather well-defined structures. The average functionality of these stars (i.e. number of arms of either kind) approaches 20 and is affected mainly by the molecular weight of the PS precursor and the molar ratio [DVB]/[LE]. To a first approximation, keeping all other experimental factors constant, it may be concluded that the higher the [DVB]/[LE] ratio and/or the lower the M_w of the linear PS precursor, the higher the functionality of the stars. A drawback of the method is that the functionality cannot be predicted theoretically at will. However, many experimental results are available and can be used to approach the desired values.

Light scattering data showed that these amphiphilic star-shaped copolymers exhibit association phenomena in water, as well as in THF which is a moderately selective solvent for the different block arms. The latter effect is very surprising and will be studied in further detail.

Finally, it has been shown that these copolymers are phase-separated in the bulk. The PEO arms can be crystallized, forming well-defined spherulites of the same kind as those appearing in block copolymers. For samples with low PEO content, this ability is strongly affected by their thermal history. These samples can be crystallized only if high supercoolings are used.

Further work is in progress in an attempt to explore the properties of these novel model macromolecules in dilute solution as well as in the solid state.

ACKNOWLEDGEMENTS

This research project was carried out within the frame of the franco–hellenic 'Platon' Programme. The authors are greatly indebted to Mr Jean-Philippe Lamps and Mrs Ourania Kouli for their kind and efficient assistance in the synthesis and characterization work. They also thank Dr Bernard Lotz of the Institute Charles Sadron for helpful discussions. Finally, the encouragement and helpful suggestions of Dr Paul Rempp are greatly appreciated.

REFERENCES

1 Tsitsilianis, C., Chaumont, P. and Rempp, P. *Makromol. Chem.* 1990, **191**, 2319
2 Tsitsilianis, C., Graff, S. and Rempp, P. *Eur. Polym. J.* 1991, **27**, 243
3 Quirk, R. P., Schock, L. E. and Lee, B. J. *Polym. Prepr. Am. Chem. Soc., Div. Polym. Chem.* 1989, **30**(1), 113
4 Berlinova, I. V. and Panayotov, I. M. *Makromol. Chem.* 1989, **190**, 1515
5 Ishizu, K. and Kuwahara, K. *J. Polym. Sci., Part A, Polym. Chem.* 1993, **31**, 661
6 Hadjichristidis, N. and Fetters, L. J. *Macromolecules* 1980, **13**, 191
7 Iatrou, H. and Hadjichristidis, N. *Macromolecules* 1992, **25**, 4649
8 Iatrou, H. and Hadjichristidis, N. *Macromolecules* 1993, **26**, 2479
9 Kanaoka, S., Omura, T., Sawamoto, M. and Higashimura, T. *Macromolecules* 1992, **25**, 6407
10 Tsitsilianis, C., Lutz, P., Gaff, S., Lamps, J.-P. and Rempp, P. *Macromolecules* 1991, **24**, 5897
11 Rein, D., Lamps, J.-P., Rempp, P., Lutz, P., Papanagopoulos, D. and Tsitsilianis, C. *Acta Polymerica* 1993, **44**, 225
12 Gnanou, Y., Lutz, P. and Rempp, P. *Makromol. Chem.* 1988, **189**, 2885
13 Berry, G. C. and Orofino, T. A. *J. Chem. Phys.* 1964, **40**, 1614
14 Flory, P. J. 'Principles of Polymer Chemistry', Cornell University Press, Ithaca, NY, 1953
15 Alliet, D. F. and Pacco, J. M. '6th GPC Seminar', Miami, FL, October 1968
16 Callot, Y., Franta, E., Benoit, H. and Rempp, P. *J. Polym. Sci (C)* 1963, **4**, 473
17 Tuzar, Z. and Kratochvil, P. *Adv. Colloid Interface Sci.* 1976, **6**, 201
18 Elias, H. G. 'Light Scattering from Polymer Solutions' (Ed. M. B. Huglin), Academic Press, London, 1972
19 De la Cruz, M. O. and Sanchez, I. C. *Macromolecules* 1986, **19**, 2501
20 Tsitsilianis, C. *Macromolecules*, 1993, **26**, 2977
21 Tsitsilianis, C., Staikos, C., Dondos, A., Lutz, P. and Rempp, P. *Polymer* 1992, **33**, 3369
22 Lotz, B. and Kovacs, A. J. *Polym. Prepr. Am. Chem. Soc., Div. Polym. Chem.* 1969, **10**, 820
23 O'Malley, J. J. *J. Polym. Sci., Polym. Symp.* 1977, **60**, 151
24 Vidotto, G., Levy, O. L. and Kovacs, A. J. *Kolloid Z., Z. Polym.* 1968, **230**, 299
25 Short, J. M. and Crystal, R. G. *Appl. Polym. Symp.* 1971, **16**, 137